A Computer Vision–Based Method for Determining the Vaccine Injection Position in Pangasius Fingerlings

Nguyen Phuc Truong[1], Luong Vinh Quoc Danh[2], Nguyen Chanh Nghiem[3]
College of Engineering, Can Tho University, Can Tho City, Vietnam[1, 2, 3]
Faculty of Electrical and Electronics Engineering, Vinh Long University of Technology Education, Vinh Long Province, Vietnam[1]

***Abstract*—Pangasius farming in the Mekong Delta is a major component of Vietnam's aquaculture industry, characterized by large-scale production, intensive farming practices, and significant contributions to export revenue. However, vaccination of Pangasius fingerlings is still predominantly performed manually, resulting in low productivity, high labor demand, and inconsistent injection accuracy, which limit large-scale deployment in commercial hatcheries. Therefore, there is an urgent need to develop an automated and accurate vaccination method for Pangasius fingerlings. This study proposes a novel computer vision–based approach for non-contact measurement of Pangasius fingerlings and accurate determination of the vaccine injection position. The proposed method leverages the image processing capabilities of the OpenCV library in combination with statistical morphological characteristics of Pangasius fingerlings to localize the injection position. The Python-implemented algorithm is lightweight and can run on an embedded Raspberry Pi platform, supporting practical in-field deployment. Experimental results demonstrate an average positioning accuracy of 97.65%, confirming the effectiveness of the proposed approach and its potential to serve as a technological foundation for automated vaccination systems in Pangasius aquaculture.**

***Keywords*—Computer vision; fish length measurement; fish vaccination; injection position; OpenCV; Pangasius**

I. Introduction

Pangasius is one of the major freshwater aquaculture products in the Mekong Delta, Vietnam, with a total export turnover of approximately USD 2 billion in 2024 [1]. Given its significant economic importance, effective disease control is essential to ensure the sustainability and competitiveness of the industry. In this context, vaccination of Pangasius fingerlings plays a crucial role in disease prevention, improving production efficiency, reducing the overuse of antibiotics, and minimizing antibiotic residues in fish products. However, vaccine injection in Pangasius fingerlings remains challenging due to their small size and morphological variability, which make accurate determination of the injection position difficult. Currently, the injection process is performed manually, resulting in low productivity, high labor demand, and inconsistent injection accuracy, as shown in Fig. 1. In addition, improper injection may damage fish internal organs and increase post-injection mortality rates. These limitations hinder large-scale and efficient vaccination in commercial hatcheries. To date, no dedicated solution has been reported that enables accurate, automated, and size-adaptive vaccination for Pangasius fingerlings. Therefore, the development of an automated and accurate vaccination method for Pangasius fingerlings is urgently required.

Fig. 1. Manual vaccination of pangasius fingerlings [2].

Motivated by these challenges, this study presents a computer vision–based approach for non-contact measurement of Pangasius fingerlings and accurate determination of the vaccine injection position. The proposed method employs image processing functions from the OpenCV library to determine the fish length. In particular, the vaccine injection position on the fish is determined based on a combination of image processing techniques and statistical data on the size and morphology of Pangasius fingerlings. For the first time, this study establishes a formulation for determining the appropriate vaccine injection position in Pangasius fingerlings using computer vision.

The organization of the present study is as follows: Section II is the review of the related literature, and Section III is the description of the proposed methodology. Section IV presents the experimental results. Section V provides concluding statements and directions for future research.

II. Related Works

Over the past two decades, the application of computer vision to fish length measurement has advanced considerably, supporting automated and non-contact measurement frameworks for modern fisheries and aquaculture systems. Among the earliest studies, White *et al.* [3] proposed the CatchMeter system, an onboard conveyor-based imaging setup that utilizes digital cameras to perform automated species classification and fish length measurement with millimeter-scale accuracy. Similarly, Jamaluddin *et al.* [4] proposed a non-contact fish length measurement system using camera-based image processing, highlighting its advantages in reducing handling stress and improving operational efficiency in aquaculture applications. The authors in [5] proposed a portable computer vision–based system using smartphone cameras and the OpenCV library to automatically measure striped catfish length, achieving an average accuracy of 97.71%. Kwon *et al.* [6] introduced a low-cost, vision-based system using dual smartphone cameras to estimate the body length and weight of olive flounder in indoor tanks with high accuracy. Lee *et al.* [7] developed an automated vision-guided Cartesian robotic system for flatfish vaccination that accurately determines injection positions under varying fish sizes and orientations.

Recent studies have integrated artificial intelligence algorithms and real-time capabilities. Tseng *et al.* [8] employed convolutional neural networks to estimate snout-to-fork length from images of harvested fish, achieving an accuracy of 95.74% in body length estimation. In [9], a stereo vision system was used to capture images of fish swimming freely in sea cages. The collected stereo data were used to train a YOLO model for simultaneous estimation of body length and weight, achieving a mean absolute percentage error of 5.5%. In [10], the authors proposed an automated framework for fish body length estimation by combining the RT-DETR deep learning model with Google ARCore technology. The system leveraged the smartphone Time-of-Flight capability to infer object distance and achieved measurement accuracy exceeding 95%. Rocha *et al.* [11] presented an automated approach for extracting morphological characteristics of freshwater fish using a Mask R-CNN framework in combination with the OpenCV library. The method estimated three body-length metrics, achieving an average relative error of 8.82% for standard length.

Despite extensive research on fish length measurement, most existing studies focus on grading, counting, or biomass estimation, while limited attention has been paid to its role in precise intervention tasks such as vaccination. In particular, research on vision-based determination of vaccine injection positions for fish fingerlings remains scarce. In addition, the substantial computational demands of deep learning frameworks restrict their adoption in cost-sensitive and resource-constraint aquaculture settings, underscoring the need for more efficient and deployable solutions. To address these limitations, this study integrates an OpenCV-based length measurement approach with statistical morphometric analysis to enable accurate and automated determination of vaccine injection positions for Pangasius fingerlings. The proposed processing pipeline is implemented in Python and can operate on embedded platforms such as Raspberry Pi, enabling practical in-field deployment.

III. Methodology

A. Image Collection

An imaging chamber was designed for acquiring images of Pangasius fingerlings. As shown in Fig. 2, the chamber consists of a Basler acA1300-200uc 1.3-megapixel camera [12] and a Raspberry Pi 4 kit with 8-GB RAM acting as the image processing unit. The images captured by the camera were transmitted to the Raspberry Pi kit [13] via a USB 3.0 interface for processing. The image processing algorithms were implemented in Python programming language (version 3.10.0) [14] using the OpenCV library (version 4.5.4.60) [15].

The fish used in this study were purchased from Pangasius farms in Vinh Long Province. The fingerlings had a body length ranging from 105 mm to 170 mm, measured from the head tip to the end of the caudal fin, and their weight ranged from 7.33 g to 35.94 g. The fish were anesthetized for imaging and morphometric measurements to establish a dataset for further analysis. The camera lens used in this study has a fixed focal length of 6 mm and an aperture of f/2.8. The fish images were captured under controlled lighting conditions at a resolution of 1280*x*1024 pixels. Prior to processing, they were resized to 800*x*600 pixels and stored in PNG format, providing a practical tradeoff between computational efficiency and measurement accuracy.

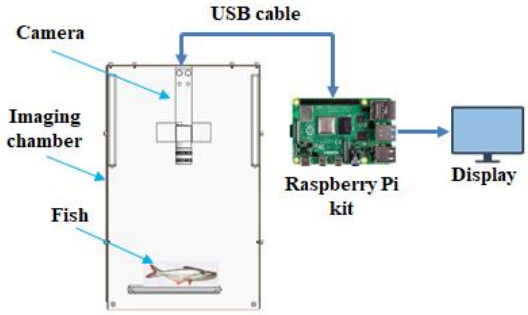

Fig. 2. Image acquisition setup.

B. Determination of the Vaccine Injection Position

The flowchart of the fish image processing procedure for determining the vaccine injection position is shown in Fig. 3. The procedure consists of seven processing steps: convert image to binary one, find contours and draw masks, extract the region of interest, determine fish orientation, find the position of fish's caudal peduncle, calculate the fish length, and determine the vaccine injection position.

1) Convert image to binary one: In this step, the original image is transformed into a binary image. The RGB image is first converted to grayscale using the OpenCV cv2.cvtColor function. Subsequently, Gaussian blurring is applied via cv2.GaussianBlur to suppress noise and smooth edges. Finally, adaptive thresholding is employed using cv2.adaptiveThreshold to convert the grayscale image into a binary image. The results of the RGB-to-binary conversion are illustrated in Fig. 4.

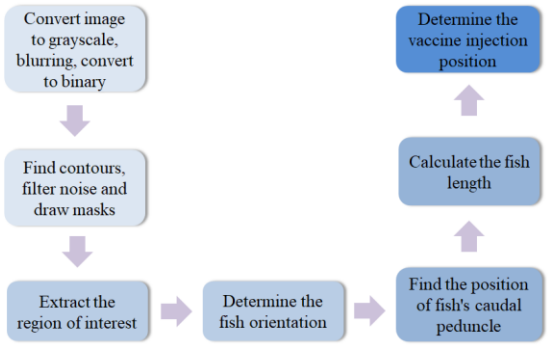

Fig. 3. The flowchart of the image processing algorithms.

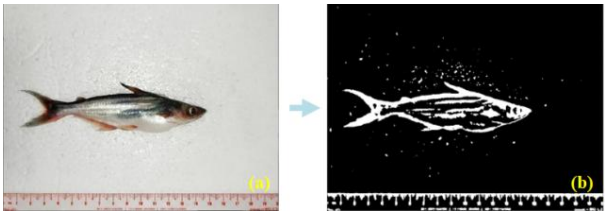

Fig. 4. Conversion from RGB to binary image: a) original RGB image; b) binary image.

2) Find contours and draw masks: In this step, object detection is performed on the binary image using the cv2.findContours function. To suppress noise, the contours.sort_contours function from the Imutils library [16] is employed to sort the detected contours and discard those with small areas. An image mask is then generated using the numpy.zeros function from the NumPy library [17] in combination with the cv2.drawContours function. The outcomes of the image masking process are presented in Fig. 5.

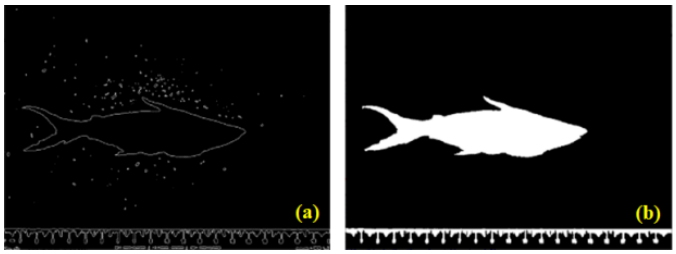

Fig. 5. Image masking: a) finding contours; b) drawing masks.

3) Extract the region of interest: The region of interest (ROI) corresponds to the image area containing the fish and is used to reduce computational cost. A rectangular ROI is extracted using the max and cv2.boundingRect functions. The extracted ROI is illustrated in Fig. 6.

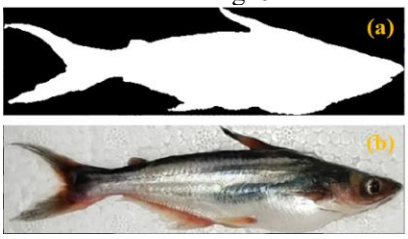

Fig. 6. Extracting the ROI: a) binary image; b) original RGB image.

4) Determine the fish orientation: During image acquisition, the fish were placed on the conveyor belt in a horizontal orientation, with their bodies aligned parallel to the direction of motion. Accordingly, two possible cases can occur: (a) the fish head is oriented to the left and (b) the fish head is oriented to the right, regardless of whether the ventral side is facing upward or downward. As shown in Fig. 7, h1 and h2 denote the heights of the fish image calculated at positions 0.2*w from the left and right boundaries of the ROI, respectively. Therefore, if h1 > h2, the fish head is oriented to the left; otherwise, the fish head is oriented to the right. For subsequent caudal peduncle detection, the ROI is transformed using the cv2.flip() function to ensure that the fish head is consistently oriented to the left, as illustrated in Fig. 8.

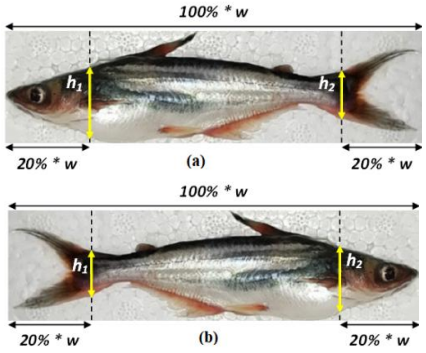

Fig. 7. Illustration of two different fish orientations: a) The fish head is oriented to the left; b) The fish head is oriented to the right.

Fig. 8. Result of changing fish orientation: a) the ROI of the binary image; b) the original image.

5) Find the position of the fish's caudal peduncle: Pangasius has a slender and elongated body that becomes narrower and flatter toward the tail. In addition, the caudal fin is thin and susceptible to damage, which can result in inaccurate length measurements. In this work, as a solution to this problem, the fish length is determined from the head tip to the narrowest region of the tail peduncle.

Fig. 9 illustrates the procedure for locating the narrowest part of the fish caudal peduncle. Specifically, the fish image ROI spanning from 0.7L to 0.9L (where L denotes the fish length) is analyzed to identify the minimum body width. A custom function, referred to as width_measuring, is developed to compute the distance between the first and last white pixels in each image column within the 0.7L÷0.9L region. The column exhibiting the minimum distance indicates the location of the narrowest part of the fish caudal peduncle. The algorithms corresponding to the proposed method are shown in Fig. 10 and Fig. 11. The outcome of this processing step is illustrated in Fig. 12.

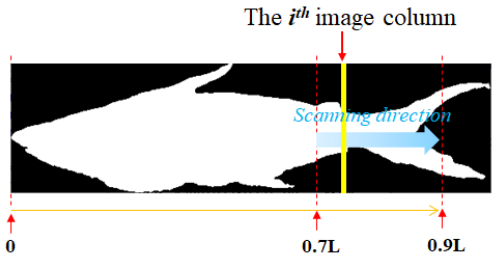

Fig. 9. Scanning for the narrowest position of the fish's caudal peduncle.

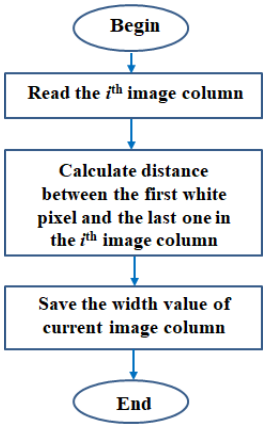

Fig. 10. The flowchart of the width_measuring function.

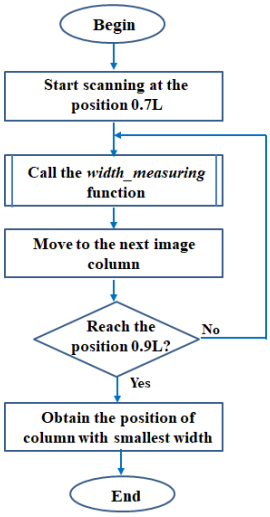

Fig. 11. Algorithm for locating the narrowest region of the fish caudal peduncle.

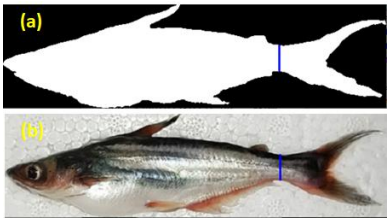

Fig. 12. Location of the narrowest part of the fish's caudal peduncle is marked with blue line in: a) the ROI of binary image and b) the original image.

6) Calculate the fish length: At this stage, the distance between the fish head tip and the location of minimum body width identified in the previous step is computed using the distance.euclidean function from the SciPy library [18]. This distance represents the fish length L, as depicted in Fig. 13, and is computed using the following Eq. (1):

$$L = N * s \quad (1)$$

where,

L: calculated fish length in millimeters.

N: the total number of image pixels located along the straight line from the fish mouth to the midpoint of the tail peduncle.

s: the physical size of a single pixel, equal to 0.264583 mm at an image resolution of 96 dpi.

Fig. 13. Determination of fish length.

7) Determine the vaccine injection position: The optimal injection needle position on the fish body is determined to be at 0.5÷0.75 of the pelvic length, anterior to the base of the pelvic fin [19]. Accordingly, the needle insertion position is point P, as illustrated in Fig. 14. The distance from the fish head tip to the injection point P, denoted as L3, is determined as follows [see Eq. (2)]:

$$L_3 = L_1 - 0.625 * L_2 \quad (2)$$

where,

L_1: the prepectoral length.

L_2: the pelvic length.

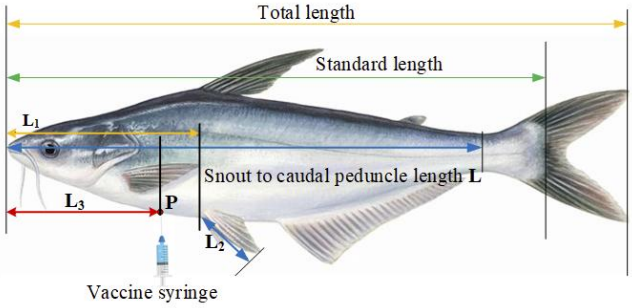

Fig. 14. Illustration of the optimal needle insertion position on the fish body.

In this study, the position of the vaccine injection point P is determined using image processing techniques in combination with experimental measurement data. Accordingly, the length L3 is determined based on Eq. (2) and the manually measured values of lengths L1 and L2.

Table I presents the experimental data from manual measurements of fish length Lm, prepectoral length *L*1, and

pelvic length L2 for 120 randomly selected Pangasius fingerlings. In Table I, R is defined as the ratio of L3 to the manually measured Lm, which corresponds to the length from the snout to the narrowest region of the caudal peduncle. Accordingly, the average value of the ratio R is determined to be 0.41.

TABLE I. MEASURED LENGTH AND WEIGHT DATA OF 120 PANGASIUS FINGERLINGS

	Manual measurement L_m: Snout to caudal peduncle length L_1: Prepectoral length L_2: Pelvic fin length L_3: Injection point w: Manual weight measurement R: Rate factor						**Image-based length measurement**	**Absolute error**	**Accuracy of image-based length measurement** $\left(100-\frac{\lvert L-L_m\rvert\cdot 100}{L_m}\right)$		**Manual measurement** L_m: Snout to caudal peduncle length L_1: Prepectoral length L_2: Pelvic fin length L_3: Injection point w: Manual weight measurement R: Rate factor						**Image-based length measurement**	**Absolute error**	**Accuracy of image-based length measurement** $\left(100-\frac{\lvert L-L_m\rvert\cdot 100}{L_m}\right)$
No.	L_m	L_1	L_2	L_3	w	R	L	$\lvert L-L_m\rvert$	(%)	No.	L_m	L_1	L_2	L_3	w	R	L	$\lvert L-L_m\rvert$	(%)
1	75.40	38.60	9.26	32.81	9.15	0.44	79.16	3.76	95.01	61	93.20	45.63	12.64	37.73	14.02	0.40	97.51	4.31	95.38
2	77.20	36.62	12.11	29.05	8.56	0.38	76.82	0.38	99.51	62	93.44	45.20	13.21	36.94	13.12	0.40	97.24	3.80	95.93
3	77.84	38.08	9.96	31.86	7.33	0.41	78.16	0.32	99.59	63	93.47	45.98	11.67	38.69	13.71	0.41	94.96	1.49	98.41
4	79.24	40.33	10.80	33.58	9.39	0.42	83.53	4.29	94.59	64	94.15	47.50	10.52	40.93	13.08	0.43	99.52	5.37	94.30
5	79.28	37.96	10.70	31.27	9.12	0.39	82.02	2.74	96.54	65	95.00	47.18	10.44	40.66	14.13	0.43	100.32	5.32	94.40
6	79.70	41.03	9.09	35.35	8.33	0.44	83.28	3.58	95.51	66	95.56	46.42	13.16	38.20	12.95	0.40	97.36	1.80	98.12
7	80.10	39.13	11.44	31.98	7.76	0.40	81.99	1.89	97.64	67	95.76	46.70	12.30	39.01	13.08	0.41	99.75	3.99	95.83
8	80.44	40.31	12.47	32.52	8.73	0.40	80.31	0.13	99.84	68	95.81	47.32	12.99	39.20	12.31	0.41	95.76	0.05	99.95
9	81.50	40.97	9.30	35.16	10.02	0.43	83.61	2.11	97.41	69	95.89	47.80	12.13	40.22	16.62	0.42	100.13	4.24	95.58
10	81.55	39.80	10.60	33.18	8.56	0.41	81.50	0.05	99.94	70	96.41	45.53	13.76	36.93	13.35	0.38	101.37	4.96	94.86
11	82.06	41.23	10.24	34.83	8.74	0.42	83.56	1.50	98.17	71	96.44	48.85	13.24	40.58	15.48	0.42	100.20	3.76	96.10
12	82.09	41.55	11.61	34.29	8.26	0.42	81.76	0.33	99.60	72	96.52	48.13	10.72	41.43	14.36	0.43	100.28	3.76	96.10
13	82.76	40.61	8.30	35.42	10.01	0.43	86.04	3.28	96.04	73	97.18	46.57	13.22	38.31	14.81	0.39	97.20	0.02	99.98
14	82.80	39.87	12.24	32.22	10.38	0.39	87.04	4.24	94.88	74	97.33	45.76	13.25	37.48	12.96	0.39	99.75	2.42	97.51
15	82.92	41.24	9.54	35.28	10.12	0.43	86.41	3.49	95.79	75	97.40	48.44	14.38	39.45	13.96	0.41	99.89	2.49	97.44
16	83.38	40.22	9.75	34.13	10.80	0.41	83.23	0.15	99.82	76	97.66	48.01	12.65	40.10	16.41	0.41	101.68	4.02	95.88
17	83.79	41.80	12.84	33.78	9.91	0.40	84.82	1.03	98.77	77	97.93	47.40	13.10	39.21	16.64	0.40	99.22	1.29	98.68
18	84.37	40.56	8.55	35.22	10.97	0.42	87.15	2.78	96.70	78	98.36	47.14	12.40	39.39	15.20	0.40	103.20	4.84	95.08
19	84.75	40.64	9.07	34.97	11.07	0.41	87.61	2.86	96.63	79	98.58	48.68	13.29	40.37	14.04	0.41	101.38	2.80	97.16
20	85.12	41.18	11.51	33.99	11.17	0.40	89.45	4.33	94.91	80	98.71	47.79	11.58	40.55	14.82	0.41	103.81	5.10	94.83
21	85.17	40.68	11.46	33.52	10.39	0.39	86.35	1.18	98.61	81	98.93	47.69	12.94	39.60	14.45	0.40	104.4	5.47	94.47
22	85.49	41.27	10.45	34.74	10.66	0.41	88.37	2.88	96.63	82	100.24	47.80	11.33	40.72	14.18	0.41	103.45	3.21	96.80
23	85.51	42.42	11.00	35.55	11.63	0.42	90.20	4.69	94.52	83	100.85	48.61	12.78	40.62	15.92	0.40	106.44	5.59	94.46
24	85.75	42.93	11.74	35.59	11.02	0.42	92.06	6.31	92.64	84	100.92	48.08	11.14	41.12	14.39	0.41	103.20	2.28	97.74
25	86.00	44.10	9.88	37.93	12.28	0.44	90.75	4.75	94.48	85	101.47	50.91	12.56	43.06	16.16	0.42	108.29	6.82	93.28

26	86.15	42.67	10.06	36.38	10.24	0.42	85.98	0.17	99.80	86	101.81	50.90	13.06	42.74	16.01	0.42	106.72	4.91	95.18
27	86.62	43.36	8.71	37.92	12.05	0.44	90.31	3.69	95.74	87	101.83	48.83	12.83	40.81	16.48	0.40	105.75	3.92	96.15
28	86.73	43.17	12.07	35.63	12.10	0.41	90.79	4.06	95.32	88	102.16	49.72	11.47	42.55	17.92	0.42	108.53	6.37	93.76
29	86.97	42.03	8.69	36.60	11.35	0.42	90.18	3.21	96.31	89	102.28	49.38	13.35	41.04	17.41	0.40	109.01	6.73	93.42
30	87.09	42.72	10.92	35.90	12.17	0.41	91.52	4.43	94.91	90	102.34	50.16	13.20	41.91	17.08	0.41	107.42	5.08	95.04
31	87.09	43.26	11.87	35.84	12.45	0.41	87.74	3.35	96.18	91	103.09	49.25	14.48	40.20	17.60	0.39	108.47	5.38	94.78
32	87.62	42.85	10.27	36.43	10.12	0.42	90.97	0.81	99.08	92	103.19	49.82	11.97	42.34	17.32	0.41	107.60	4.41	95.73
33	87.70	43.60	8.82	38.09	11.97	0.43	88.51	5.73	93.47	93	103.34	50.16	14.34	41.20	18.87	0.40	106.79	3.45	96.66
34	87.71	44.78	11.23	37.76	11.78	0.43	93.44	2.95	96.64	94	103.54	48.96	11.58	41.72	17.83	0.40	108.78	5.24	94.94
35	87.86	43.63	10.20	37.26	11.57	0.42	90.81	4.39	95.01	95	104.13	50.58	15.30	41.02	17.77	0.39	109.16	5.03	95.17
36	87.96	44.38	12.11	36.81	12.64	0.42	92.35	2.50	97.16	96	104.37	51.13	14.23	42.24	17.31	0.40	110.68	6.31	93.95
37	87.98	43.57	11.04	36.67	11.30	0.41	90.48	1.66	98.13	97	105.13	51.41	11.55	44.19	16.82	0.42	110.98	5.85	94.44
38	88.85	43.81	12.51	35.99	12.26	0.40	90.51	2.00	97.75	98	105.18	51.19	14.47	42.15	18.14	0.40	111.14	5.96	94.33
39	88.89	44.11	10.46	37.57	13.37	0.42	90.89	3.81	95.71	99	105.96	51.59	11.90	44.15	18.91	0.42	109.94	3.98	96.24
40	88.89	43.01	12.29	35.33	11.21	0.40	92.72	1.50	98.32	100	106.76	51.55	11.30	44.49	18.27	0.42	112.00	5.24	95.09
41	89.37	43.05	12.86	35.01	11.53	0.39	90.87	5.87	93.43	101	106.96	51.87	11.80	44.50	18.33	0.42	112.72	5.76	94.61
42	89.37	44.75	12.04	37.23	11.91	0.42	95.26	5.07	94.33	102	107.03	51.45	13.84	42.80	18.93	0.40	113.13	6.10	94.30
43	89.45	44.44	13.17	36.21	12.69	0.40	94.52	5.36	94.01	103	107.39	50.91	13.47	42.49	19.26	0.40	113.93	6.54	93.91
44	89.54	42.96	11.82	35.57	13.31	0.40	94.90	5.20	94.20	104	108.76	51.55	11.25	44.52	17.92	0.41	115.25	6.49	94.03
45	89.61	42.37	11.31	35.30	11.47	0.39	94.81	1.57	98.25	105	108.87	53.77	13.18	45.53	21.21	0.42	113.35	4.48	95.89
46	89.95	44.06	11.17	37.08	14.45	0.41	91.52	4.98	94.47	106	109.75	53.13	11.64	45.86	18.38	0.42	116.71	6.96	93.66
47	90.06	44.17	11.23	37.15	13.82	0.41	95.04	4.55	94.96	107	109.91	52.93	14.79	43.69	18.79	0.40	116.08	6.17	94.39
48	90.30	44.95	12.66	37.04	12.04	0.41	94.85	0.87	99.04	108	110.54	55.63	13.79	47.01	20.32	0.43	114.73	4.19	96.21
49	90.32	44.28	11.87	36.86	13.56	0.41	91.19	3.34	96.31	109	111.16	52.87	14.06	44.08	21.22	0.40	114.83	3.67	96.70
50	90.40	44.68	11.84	37.28	14.36	0.41	93.74	5.38	94.07	110	112.86	54.77	15.23	45.25	23.35	0.40	117.89	5.03	95.54
51	90.67	43.21	12.02	35.70	12.17	0.39	96.05	0.48	99.47	111	114.45	53.92	13.96	45.20	22.82	0.39	120.12	5.67	95.05
52	91.04	44.24	11.12	37.29	11.74	0.41	91.52	4.50	95.08	112	116.19	54.93	12.70	46.99	25.22	0.40	122.90	6.71	94.22
53	91.40	43.69	12.13	36.11	12.94	0.39	95.90	4.70	94.86	113	116.79	55.90	16.21	45.77	23.10	0.39	121.57	4.78	95.91
54	91.42	45.51	12.11	37.94	12.99	0.41	96.12	1.83	98.00	114	117.16	57.49	13.21	49.23	24.15	0.42	122.50	5.34	95.44
55	91.63	45.24	12.52	37.42	14.17	0.41	93.46	4.47	95.13	115	121.54	57.94	16.76	47.47	26.76	0.39	129.66	8.12	93.32
56	91.85	43.80	10.65	37.14	12.49	0.40	96.32	3.90	95.76	116	122.28	59.76	17.62	48.75	34.55	0.40	131.14	8.86	92.75
57	91.88	44.76	12.03	37.24	14.15	0.41	95.78	4.63	94.96	117	122.58	59.36	16.01	49.35	32.26	0.40	129.71	7.13	94.18
58	91.91	45.69	13.34	37.35	13.49	0.40	96.54	2.45	97.35	118	125.85	61.67	16.86	51.13	28.92	0.41	132.14	6.29	95.00
59	92.50	47.11	12.82	39.10	13.58	0.42	94.95	4.19	95.47	119	126.70	63.03	16.54	52.69	35.26	0.42	133.88	7.18	94.33
60	92.52	45.34	11.63	38.07	13.15	0.41	96.71	2.27	97.55	120	133.27	61.74	15.72	51.92	35.94	0.39	138.95	5.68	95.74

As shown in Table I, the absolute error between the fish length measured using image processing L and that obtained by manual measurement L_m ranges from a minimum of 0.02 mm to a maximum of 8.86 mm, with an average error of 3.92 mm (i.e., 4%). This error may result from inaccuracies in manual measurements and in pixel-count calculations on the fish image.

Based on the statistical data in Table I, the correlation between the manually measured fish length L_m and the image-derived fish length L was obtained using the Matlab curve fitting toolbox [20] with a coefficient of determination R^2 = 0.9856, as shown in Fig. 15 and expressed by Eq. (3):

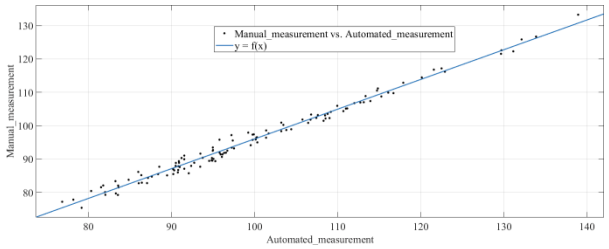

Fig. 15. Correlation function between L_m and L.

$$L_m = 0.8907 * L + 6.975 \quad (3)$$

In summary, the vaccine injection point on the fish P is defined by the distance from the fish head tip to P, denoted as $L_{injection}$, which is computed as follows:

$$L_{injection} = 0.41 * (0.8907 * L + 6.975) \quad (4)$$

Based on the fish length determined using image processing techniques and Eq. (4), the microprocessor can control the vaccine syringe to move to the determined injection point.

8) Fish weight estimation: From the statistical survey results of fish length L_m and the corresponding weight W in Table I, the fish weight can be estimated as a function of fish length with a coefficient of determination R^2 = 0.9502, and is expressed by the following Eq. (5):

$$W = 0.0000617y^3 - 0.01268y^2 + 1.1y - 29.07 \quad (5)$$

where, y is the fish length calculated from Eq. (3).

IV. Experimental Results

To verify the effectiveness and accuracy of the proposed method, 65 Pangasius fingerlings with weights ranging from 6.52 g to 41.3 g were randomly selected for validation. The fingerlings were reared in tanks and anesthetized prior to measurement. Fish size measurements were then conducted using two methods: using a digital caliper and an image-based method, as shown in Fig. 16. The comparison results between image-based measurements and manual measurements are presented in Table II. The experimental results indicate that the calculated fish length data exhibit an average absolute error of 0.94 mm, with accuracy ranging from 96.79% to 99.96%, and an average accuracy of 99.05%. The injection position estimation results show an average absolute error of 1 mm and an average accuracy of 97.65%. In addition, the fish weight estimation results achieve an average accuracy of 93.75% with an average absolute error of 2.66 g. The average processing time from image capture to result display is 0.25 seconds.

The accuracy of fish length, injection position, and weight estimations is computed as given in Eq. (6), Eq. (7), and Eq. (8), respectively:

$$Fish\ length\ accuracy = 100 - \frac{|L - L_m|}{L_m} * 100 \quad (6)$$

$$Injection\ accuracy\ (\%) = 100 - \frac{|L_{injection} - L_3|}{L_3} * 100 \quad (7)$$

$$Weight\ accuracy\ (\%) = 100 - \frac{|W_i - W_m|}{W_m} * 100 \quad (8)$$

TABLE II. Experimental Measurement Results

No.	Snout to caudal peduncle length measurement		Weight		Prepectoral length	Pelvic fin length	Injection point		Absolute errors			Accuracy (%)		
	Manual (L_m)	Image-based (L)	Manual (W_m)	Image-based (W_i)	Manual measurement (L_1)	Manual measurement (L_2)	Manual measurement (L_3)	Image-based measurement $L_{injection}$	$\lvert L - L_m \rvert$	$\lvert W_i - W_m \rvert$	$\lvert L_{injection} - L_3 \rvert$	$100 - \frac{\lvert L - L_m \rvert}{L_m} * 100$ Length	$100 - \frac{\lvert W_i - W_m \rvert}{W_m} * 100$ Weight	$100 - \frac{\lvert L_{injection} - L_3 \rvert}{L_3} * 100$ Injection point
1	75.21	74.30	6.55	7.97	37.56	9.69	31.50	30.46	0.91	1.42	1.04	98.79	78.32	96.70
2	79.19	81.26	8.98	9.69	38.89	9.50	32.95	33.32	2.07	0.71	0.36	97.39	92.09	98.88
3	79.77	78.26	6.52	8.93	39.09	10.73	32.38	32.09	1.51	2.41	0.30	98.11	63.04	99.10
4	81.54	83.09	10.11	10.18	40.30	9.07	34.63	34.07	1.55	0.07	0.56	98.10	99.31	98.38
5	82.19	81.46	9.25	9.75	40.46	10.46	33.92	33.40	0.73	0.50	0.53	99.11	94.59	98.47
6	83.38	82.87	9.94	10.12	40.34	11.64	33.07	33.98	0.51	0.18	0.91	99.39	98.19	97.25
7	84.54	83.82	10.88	10.38	40.84	10.73	34.13	34.37	0.72	0.50	0.23	99.15	95.40	99.30
8	85.43	84.54	11.01	10.58	42.38	11.56	35.16	34.66	0.89	0.43	0.49	98.96	96.09	98.58

9	85.97	87.34	11.21	11.36	43.39	11.59	36.15	35.81	1.36	0.15	0.34	98.41	98.66	99.06
10	86.68	87.72	11.54	11.50	41.80	12.72	33.85	35.96	1.04	0.04	2.11	98.80	99.65	93.77
11	87.53	85.13	10.86	10.74	42.86	10.54	36.27	34.90	2.40	0.12	1.37	97.26	98.90	96.22
12	87.86	85.54	10.63	10.86	42.52	11.30	35.46	35.07	2.32	0.23	0.38	97.36	97.84	98.90
13	88.47	88.75	11.16	11.81	42.91	12.06	35.37	36.39	0.28	0.65	1.02	99.68	94.18	97.12
14	89.36	90.23	11.96	12.27	43.52	12.16	35.92	36.99	0.87	0.31	1.07	99.03	97.41	97.02
15	89.51	87.62	11.04	11.47	43.13	12.38	35.39	35.92	1.89	0.43	0.53	97.89	96.11	98.50
16	89.97	90.88	13.93	12.48	44.03	9.65	38.00	37.26	0.91	1.45	0.74	98.99	89.59	98.05
17	90.39	87.49	11.62	11.43	43.61	11.69	36.30	35.87	2.90	0.19	0.43	96.79	98.36	98.82
18	91.20	92.06	14.08	12.87	44.06	10.92	37.24	37.75	0.86	1.21	0.51	99.06	91.41	98.63
19	91.82	91.44	14.59	12.67	42.16	11.81	34.78	37.49	0.38	1.92	2.71	99.59	86.84	92.21
20	92.38	92.79	13.28	13.12	44.92	10.40	38.42	38.04	0.41	0.16	0.38	99.56	98.80	99.01
21	92.99	93.34	13.93	13.31	44.96	10.33	38.50	38.27	0.35	0.62	0.24	99.62	95.55	99.40
22	93.94	92.19	12.69	12.91	46.89	14.48	37.84	37.80	1.75	0.22	0.04	98.14	98.27	99.89
23	95.65	94.41	14.35	13.68	48.81	11.71	41.49	38.71	1.24	0.67	2.78	98.70	95.33	93.30
24	95.89	94.90	13.86	13.86	47.76	10.66	41.10	38.91	0.99	0.00	2.19	98.97	100.00	94.67
25	96.95	95.66	13.93	14.13	49.31	12.22	41.67	39.22	1.29	0.20	2.45	98.67	98.56	94.12
26	97.49	98.21	14.56	15.11	47.16	11.69	39.85	40.27	0.72	0.55	0.41	99.26	96.22	98.95
27	98.37	97.80	12.53	14.94	48.74	13.47	40.32	40.10	0.57	2.41	0.22	99.42	80.77	99.45
28	99.65	99.61	15.13	15.67	49.37	9.93	43.16	40.84	0.04	0.54	2.32	99.96	96.43	94.62
29	101.27	101.85	16.89	16.62	48.81	13.49	40.38	41.76	0.58	0.27	1.38	99.43	98.40	96.58
30	102.12	102.45	16.15	16.88	49.52	13.62	41.01	42.00	0.33	0.73	1.00	99.68	95.48	97.59
31	102.75	103.13	17.42	17.19	50.16	13.10	41.97	42.28	0.38	0.23	0.31	99.63	98.68	99.26
32	103.36	102.67	16.40	16.98	51.37	14.49	42.31	42.10	0.69	0.58	0.22	99.33	96.46	99.50
33	104.82	104.15	16.94	17.66	49.18	14.33	40.22	42.70	0.67	0.72	2.48	99.36	95.75	93.83
34	106.21	105.63	17.58	18.36	53.19	15.55	43.47	43.31	0.58	0.78	0.16	99.45	95.56	99.63
35	106.60	106.47	18.92	18.78	54.72	14.99	45.35	43.65	0.13	4.14	1.70	99.88	99.26	96.25
36	107.28	107.61	20.82	19.35	52.09	13.12	43.89	44.12	0.33	1.47	0.23	99.69	92.94	99.48
37	108.91	109.09	19.90	20.13	54.27	15.48	44.60	44.73	0.18	3.77	0.13	99.83	98.84	99.71
38	109.06	109.76	18.96	20.49	52.14	13.73	43.56	45.00	0.70	1.53	1.44	99.36	91.93	96.69
39	109.91	110.87	23.78	21.11	56.71	15.96	46.74	45.46	0.96	6.67	1.28	99.13	88.77	97.26
40	110.15	111.28	21.10	21.34	55.93	15.95	45.96	45.62	1.13	3.76	0.34	98.97	98.86	99.26
41	110.29	111.18	21.45	21.28	56.97	15.12	47.52	45.58	0.89	4.17	1.94	99.19	99.21	95.92
42	110.69	110.22	20.30	20.74	55.13	16.88	44.58	45.19	0.47	0.44	0.61	99.58	97.83	98.63
43	110.73	111.38	21.05	21.40	54.75	15.26	45.21	45.67	0.65	3.65	0.46	99.41	98.34	98.98
44	110.85	110.53	25.27	20.92	54.97	16.74	44.51	45.32	0.32	8.35	0.81	99.71	82.79	98.18
45	111.80	111.22	21.53	21.31	55.94	15.77	46.08	45.60	0.58	4.22	0.48	99.48	98.98	98.96
46	113.63	115.01	23.90	23.58	58.52	14.35	49.55	47.15	1.38	4.32	2.40	98.79	98.66	95.16
47	113.70	114.65	22.57	23.35	57.94	15.59	48.20	47.01	0.95	3.22	1.19	99.16	96.54	97.53
48	113.76	113.54	25.22	22.67	58.83	16.09	48.77	46.55	0.22	6.55	2.22	99.81	89.89	95.45
49	114.12	113.41	23.19	22.59	56.61	16.31	46.42	46.50	0.71	4.60	0.08	99.38	97.41	99.83
50	114.77	113.46	26.06	22.62	57.48	16.48	47.18	46.52	1.31	7.44	0.66	98.86	86.80	98.60
51	115.06	115.14	25.73	23.66	56.15	14.82	46.89	47.21	0.08	2.07	0.32	99.93	91.95	99.32
52	115.63	114.93	23.98	23.53	58.26	17.18	47.52	47.12	0.70	4.45	0.40	99.39	98.12	99.16
53	116.53	116.81	25.40	24.75	59.67	15.97	49.69	47.89	0.28	4.65	1.80	99.76	97.44	96.38
54	117.41	116.57	25.02	24.59	57.98	16.85	47.45	47.79	0.84	4.43	0.34	99.28	98.28	99.28
55	117.62	116.32	27.81	24.42	58.67	16.39	48.43	47.69	1.30	7.39	0.74	98.89	87.81	98.47
56	118.43	119.12	27.26	26.33	60.36	15.43	50.72	48.84	0.69	4.93	1.88	99.42	96.59	96.29
57	118.72	117.04	27.45	24.90	59.50	15.73	49.67	47.99	1.68	6.55	1.68	98.58	90.71	96.62
58	119.96	121.64	25.10	28.17	60.53	17.22	49.77	49.87	1.68	0.93	0.10	98.60	87.77	99.80
59	120.54	117.49	26.23	25.20	56.90	15.47	47.23	48.17	3.05	1.03	0.94	97.47	96.07	98.01
60	121.02	120.19	30.49	27.09	62.02	17.16	51.30	49.28	0.83	7.40	2.02	99.31	88.85	96.06
61	122.04	121.45	31.74	28.02	62.10	17.08	51.43	49.79	0.59	7.72	1.64	99.52	88.28	96.81
62	123.63	122.39	34.61	28.74	61.04	19.15	49.07	50.18	1.24	9.87	1.11	99.00	83.04	97.74
63	123.85	123.67	31.59	29.74	62.22	16.92	51.65	50.70	0.18	5.85	0.95	99.85	94.14	98.16
64	125.28	126.73	41.30	32.27	60.13	13.88	51.46	51.96	1.45	9.03	0.50	98.84	78.14	99.03
65	128.95	130.15	37.89	35.33	66.64	17.10	55.95	53.36	1.20	6.56	2.59	99.07	93.24	95.37

Fig. 16. Conducting fish length measurements: a) Pangasius fingerlings tank; b) Fish were anesthetized prior to measurement; c) Manual measurement using digital caliper; d) Image-based measurement using computer vision.

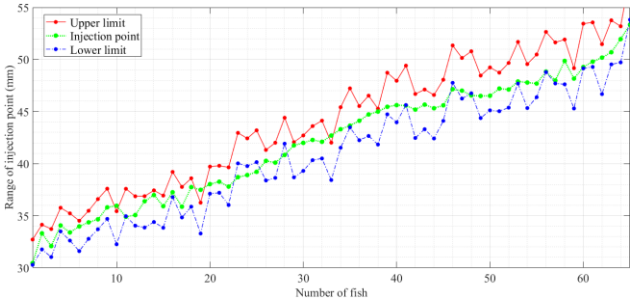

Fig. 17. Calculated results of the vaccine injection position.

The results of the vaccine injection position estimation and the practical injection tolerance range are illustrated in Fig. 17. The experimental data show that most of the calculated injection positions fall within the allowable limits, except for three cases with deviations greater than 1 mm, which are 1.32 mm, 1.24 mm, and 1.08 mm, respectively. In practice, it has also been observed that some Pangasius fingerlings have different pelvic fin lengths despite having the same body length. This may be one of the causes of the observed discrepancies. Besides, the use of a camera equipped with a short-focal-length lens (6 mm, f/2.8) introduces spatial nonuniformity in pixel density, which also contributes to measurement deviations. However, these errors remain within acceptable limits for practical implementation. The proposed method offers a more accurate and reliable approach to automated injection than manual vaccination, where high-intensity human operation can introduce errors that compromise post-injection fish health.

V. Conclusion and Future Work

This study has proposed and experimentally validated a novel computer vision–based approach for accurately determining the vaccine injection position in Pangasius fingerlings. By leveraging the image processing capabilities of the OpenCV library in combination with statistical morphological data of Pangasius fingerlings, the proposed method achieved an average accuracy of 97.65%. The open-source Python-based pipeline operates on embedded platforms, enabling practical in-field deployment. This work is the first to establish a computer-vision–based formulation for locating the vaccine injection position in Pangasius fingerlings. The results demonstrate the feasibility of applying computer vision techniques to support automated vaccination tasks for Pangasius fingerlings.

The estimation accuracy of the image-based approach can be further improved by optimizing the illumination conditions within the imaging chamber and by selecting a camera lens with a focal length appropriate for the fish size. Future work will focus on integrating the proposed vision-based measurement approach with mechatronic actuators and an embedded control system toward a fully automated vaccination platform. Such integration is expected to increase throughput, improve injection consistency, and substantially reduce labor costs in commercial Pangasius hatcheries.

Acknowledgment

The authors would like to sincerely thank Assoc. Prof. Tu Thanh Dung, College of Aquaculture and Fishery, Can Tho University, for her valuable advice on vaccination techniques for Pangasius fingerlings.

Declaration on Generative AI

The authors acknowledge using ChatGPT to improve the clarity and grammar of the manuscript. The content, analysis, and conclusions remain the sole responsibility of the authors.

References

[1] Vietnam News. Vietnam's pangasius exports expected to reach $2b in 2024. https://vietnamnews.vn/economy/1687381/viet-nam-s-pangasius-exports-expected-to-reach-2b-in-2024.html

[2] Hien La. Vaccines and a vision for sustainable development in pangasius farming. https://tepbac.com/tin-tuc/full/vac-xin-va-tam-nhin-phat-trien-ben-vung-trong-nghe-nuoi-ca-tra-33297.html (in Vietnamese)

[3] D.J. White, C. Svellingen, N.J.C. Strachan, "Automated Measurement of Species and Length of Fish by Computer Vision". Fisheries Research, Volume 80, Issues 2–3, 203-210 (2006).

[4] Jamaluddin, M. H., Siong Seng, C., Shukor, A. Z., Ali Ibrahim, F., Miskon, M. F., Mohd Aras, M. S., Md Ghazaly, M., & Ranom, R., "The Effectiveness of Fish Length Measurement System using Non-Contact Measuring Approach". Jurnal Teknologi, 77(20) (2015).

[5] L. H. Phong, N. P. Truong, L. V. Q. Danh, V. H. Nam, N. T. Tung, and T. T. Dung, "A Portable System for Automated Measurement of Striped Catfish Length Using Computer Vision," in Ubiquitous Intelligent Systems, Singapore, P. Karuppusamy, F. P. García Márquez, and T. N. Nguyen, Eds., 2022// 2022: Springer Nature Singapore, pp. 607-618.

[6] Kwon, Inyeong, Hang Thi Phuong Nguyen, Paththige Waruni Prasadini Fernando, Hieyong Jeong, Sungju Jung, and Taeho Kim. "Prototype Mobile Vision System for Automatic Length Estimation of Olive Flounder (Paralichthys olivaceus) in Indoor Aquaculture" Journal of Marine Science and Engineering, 2025, 13, no. 6: 1167. https://doi.org/10.3390/jmse13061167.

[7] Lee D. G., Bong-Jin Cha, Seong-Wook Park, Mun-Gyeong Kwon, Guo-Cheng Xu, Hee-Je Kim, "Development of a vision-based automatic vaccine injection system for flatfish,". Aquacultural Engineering, Volume 54, 2013, pages 78-84, ISSN 0144-8609, https://doi.org/10.1016/j.aquaeng.2012.12.001.

[8] Tseng C. H, Ching-Lu Hsieh, Yan-Fu Kuo. "Automatic measurement of the body length of harvested fish using convolutional neural networks," Biosystems Engineering, Volume 189, 2020, Pages 36-47, ISSN 1537-5110.

[9] Tonachella, N., Martini, A., Martinoli, M. et al. "An affordable and easy-to-use tool for automatic fish length and weight estimation in

mariculture". Sci Rep 12, 15642 (2022). https://doi.org/10.1038/s41598-022-19932-9.

[10] Kang, Seung-Beom, Seung-Gyu Kim, Sang-Hyun Lee, and Tae-Ho Im. "A Study on the Automation of Fish Species Recognition and Body Length Measurement System," Fishes, 2024, no. 9: 349. https://doi.org/10.3390/fishes9090349

[11] Rocha, W.S., da Fonseca, T.F.C., Watanabe, C.Y.V. et al. "Automatic measurement of fish from images using convolutional neural networks,". Multimedia Tools and Applications, 84, 6327–6347 (2025). https://doi.org/10.1007/s11042-024-19180-1

[12] Basler ace. acA1300-200uc. https://www.baslerweb.com/en/shop/aca1300-200uc/

[13] Raspberry Pi 4. https://www.raspberrypi.com/products/raspberry-pi-4-model-b/

[14] Python. https://www.python.org/downloads/

[15] OpenCV library. https://opencv.org

[16] Imutils library. https://pypi.org/project/imutils

[17] Numpy library. https://numpy.org

[18] Scipy library. https://scipy.org

[19] Pharmaq. Vaccine Package Insert. (2018). https://pharmaq-cdn-e9g8bdeng6hhcsee.z01.azurefd.net/media/njgph0sn/pil-ajpanga2-vn-v3-english.pdf

[20] Matlab. Curve fitting toolbox. https://www.mathworks.com/products/curvefitting.html